Impact of ENSO on seasonal variations of Kelvin Waves and mixed Rossby-Gravity Waves

2017 IOP Conf. Ser.: Earth Environ. Sci. 54 012035

(http://iopscience.iop.org/1755-1315/54/1/012035)

Impact of ENSO on seasonal variations of Kelvin Waves and mixed Rossby-Gravity Waves

Saeful Rakhman[1]*, Sandro W Lubis[2] and Sonni Setiawan[1]
[1]Department of Geophysics and Meteorology, Bogor Agricultural University (IPB), Indonesia
[2]Physics of the Atmoshpere, GEOMAR Helmholtz Centre for Ocean Research Kiel, Germany

E-mail: saefulrakhman88@gmail.com

Abstract. Characteristics of atmospheric equatorial Kelvin waves and mixed Rossby-Gravity (MRG) waves as well as their relationship with tropical convective activity associated with El Niño-Southern Oscillation (ENSO) were analyzed. Kelvin waves and MRG waves were identified by using a Space-Time Spectral Analysis (STSA) technique, where the differences in the strength of both waves were quantified by taking the wave spectrum differences for each ENSO phase. Our result showed that Kelvin wave activity is stronger during an El Nino years, whereas the MRG wave activity is stronger during the La Nina years. Seasonal variations of Kelvin wave activity occurs predominantly in MAM over the central to the east Pacific in the El Nino years, while the strongest seasonal variation of MRG wave activity occus in MAM and SON over the northern and southern Pacific during La Nina years. The local variation of Kelvin wave and MRG wave activities are found to be controlled by variation in lower level atmospheric convection induced by sea surface temperature in the tropical Pacific Ocean.

1. Introduction

Equatorial planetary waves (EPW) are one of the dominant modes of synoptic-to-subseasonal variability in the tropics. They are generated by diabatic heating due to organized tropical large-scale convective heating in the equatorial belt [1][2][3]. The amplitude is captured clearly in the equatorial belt between 20°N and 20°S [1]. EPW causes predominant disturbances in the equatorial atmosphere such as inducing mean-meridional circulation that is important for the heat balance of the equatorial belt [4][5], affecting the patterns of low level moisture convergence, and controling the distribution of tropical convective heating and storms in large longitudinal distances [4]. In addition, EPW also plays an important role in modulating rainfall in the tropics [3], circulation Walker [6], Madden and Julian oscillation (MJO) [7] and El Nino-Southern Oscillation (ENSO) [5]. Two dominant atmospheric equatorial waves has an important role in the region is equatorial Kelvin waves and Mixed Rossby-Gravity (MRG) waves. In this study our analysis will focus on understanding the nature of Kelvin waves and MRG waves during ENSO events.

El Niño Southern Oscillation (ENSO) is a coupled atmosphere-ocean phenomenon characterized by anomalous ocean warming over the eastern equatorial Pacific ocean [8]. ENSO can be classified into normal, El Niño and La Niña phases. The term El Niño refers to a large-scale periodic warming in sea surface temperatures across the central and east-central Equatorial Pacific. On the other hand, La Niña represent periods of below-average sea surface temperatures across the east-central Equatorial

Pacific. This phenomenon affects the climate over sizable portions of the globe, including some regions far removed from the tropical Pacific Ocean [9].

Warming in the tropical ocean (i.e., increased sea surface temperature – SST) will increase the evaporation and hence, the formation of large scale convective clouds. The process causes latent heating in the upper atmosphere which is very important ingredient to generate more EPW activity [10]. Kelvin waves and MRG waves are well observed within the anomalies of SST, precipitation, and outgoing longwave radiation (OLR) in the tropics [3]. Therefore, in this study we used both SST and OLR datasets as a proxy to isolate the Kelvin wave and MRG wave activity. The goal of the current study is to investigate the impact of ENSO on seasonal variation of Kelvin wave and MRG waves and the involved mechanisms.

2. Methods

ENSO phases were identified by using Running 3-month ONI Mean Values data. Sea surface temperature profile data is displayed using the NCEP Optimum Interpolation Sea Surface Temperature (OISST) in the period from 1982 to 2013 and a spatial resolution of 1° x 1°. In addition, OLR profile displayed using daily interpolated of outgoing longwave radiation (OLR) data in the period from 1974 to 2013 from National Oceanic and Atmospheric Administration (NOAA) Global CPC (except 1978). Details interpolation technique can be seen in the OLR data [11]. Horizontal wind datasets (u,v) at an altitude of 1000 hPa and 850 hPa and vertical velocity (ω) in the troposphere (1000 hPa-100 hPa) from National Centre for Environmental Prediction (NCEP/NCAR reanalysis 1: Pressure) each at 20°N-20°S in the equatorial bands with a spatial resolution of 2.5° x 2.5°.

2.1. Composite Analysis

Composite analysis is a method used to determine the field distribution of certain atmospheric conditions. In this study, composite analysis is used to analyze the distribution of sea surface temperature, outgoing longwave radiation and vertical velocity for each phase of ENSO. Composite technique is nothing but the ensemble average, the average value is calculated from a set of data, but in the same condition.

2.2. Space-Time Spectral Analysis (STSA)

STSA is one of the methodology that been used in this study. STSA is a method used to analyze the wave propagation in the zonal field. This method decomposing the physical data field in the domain of space and time into a data field in the domain of wavenumber and frequency of the waves that propagate to westward and eastward [12]. In principle, this decomposition process is the Fourier transform of the data in space and time domain into data in frequency (ω) and wavenumber (k) domain. STSA procedure contained in NCL software (NCAR Command Language) with SpaceTime function. The output of this method is the contours of the power spectrum that contained in the dispersion curve as a function of frequency and zonal wavenumber that classified into symmetric and asymmetric components.

3. Result

3.1. Identification Phase of ENSO

ENSO occurrences in this study were identified using Nino 3.4 index. The index is an index based on the average of sea surface temperature anomalies (SST) in 5°S-5°N, 120°-170°W. Nino 3.4 index 3-month running average of the period 1974 to 2013 (figure 1). The number of events each ENSO phase are listed in Table 1.

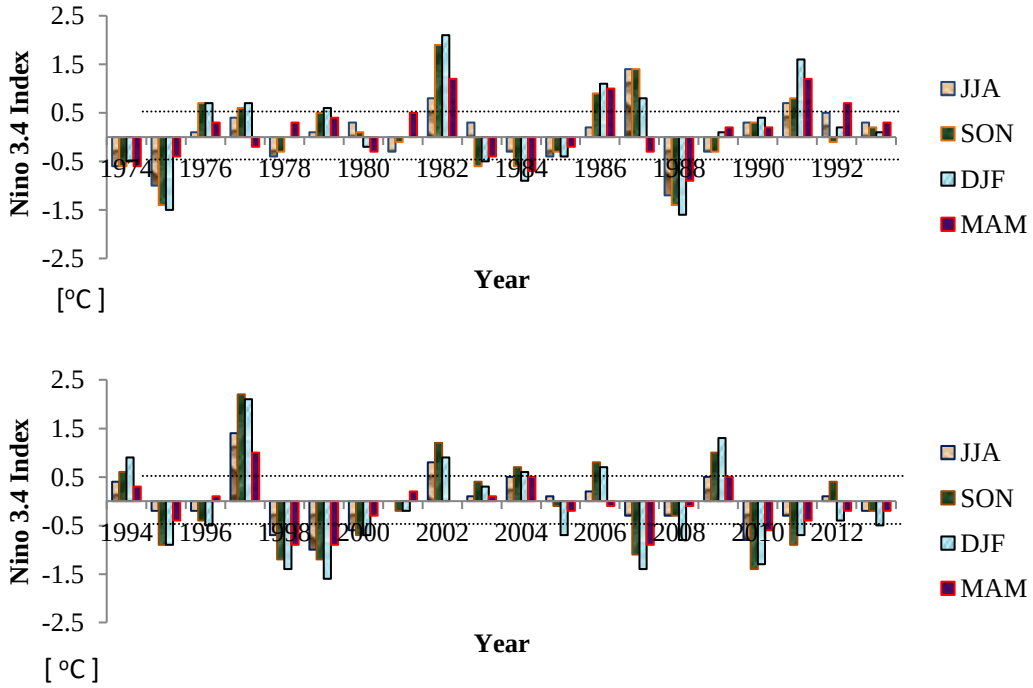

Figure 1. Average of 3-month run of sea surface temperature anomalies (SST,°C) Nino 3.4 index from 1974 to 2013.

Table 1. Season Number of events at each phase of ENSO (1974-2013)

Condition	**DJF**	**MAM**	**JJA**	**SON**
Normal	12	25	25	15
El Nino	13	8	8	13
La Nina	15	7	7	12

3.2. Seasonal Variations of Kelvin Wave and Mixed Rossby-Gravity (MRG) Wave at each Phase of ENSO

Identification of the equatorial planetary wave activity (EPW) were calculated using STSA [12]. The data used is the average of the daily OLR anomalies for ~ 40 years (1974-2013) on 15°LU-15°LS. Previously, the data is grouped into seasons for each phase of ENSO. Results of STSA OLR with an effective depth of 12-50 m are selected is shown in figure 2 (Symetric Component) and figure 3 (Antisymetric Component). The black box shows the waves become the focus of study in this research.

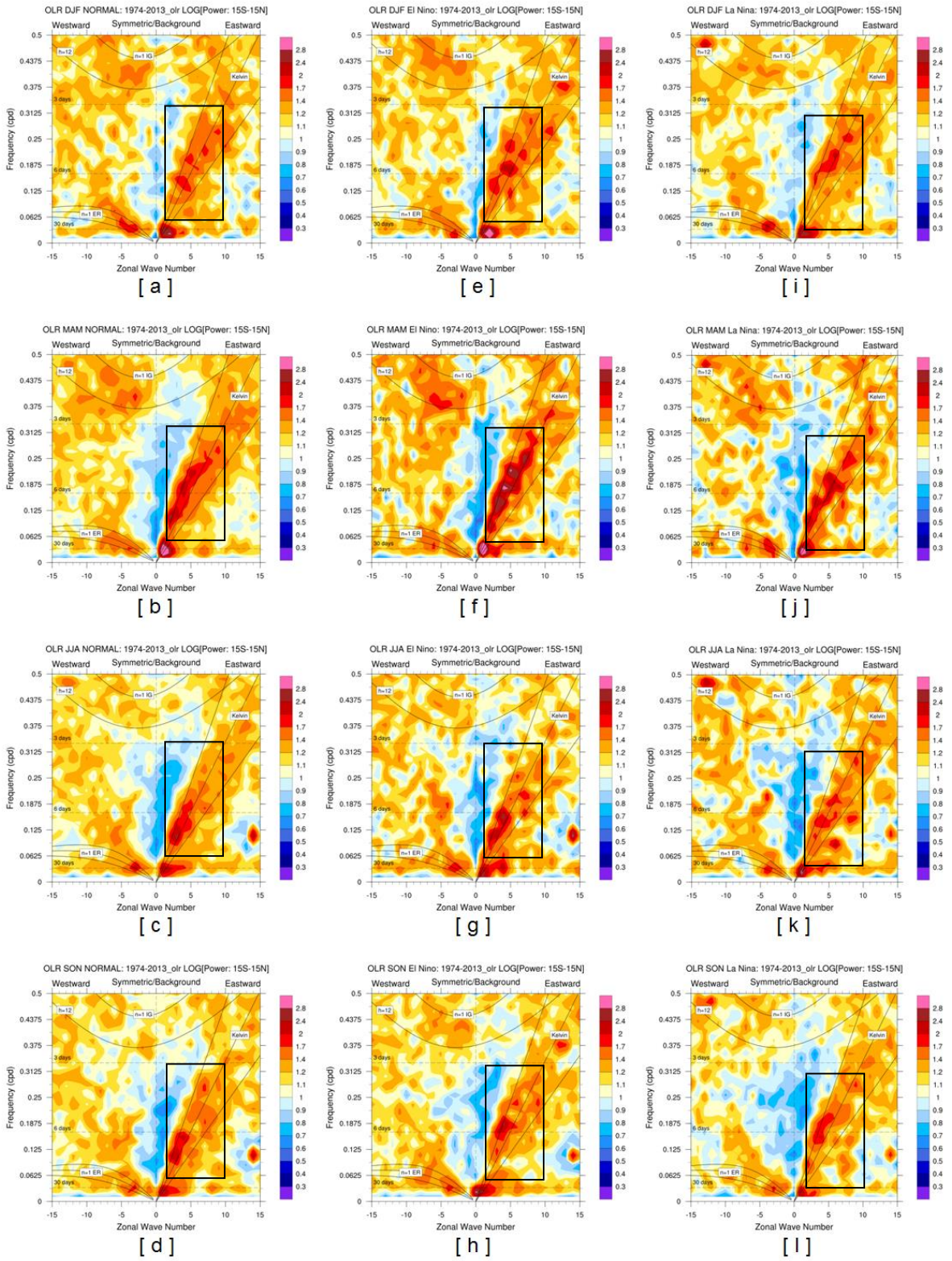

Figure 2. Symmetric STSA of outgoing longwave radiation in the normal phase (DJF (a), MAM (b), JJA (c), SON (d)), El Nino phase (DJF (e), MAM (f), JJA (g), SON (h)), La Nina phase (DJF (i), MAM (j), JJA (k), SON (l)).

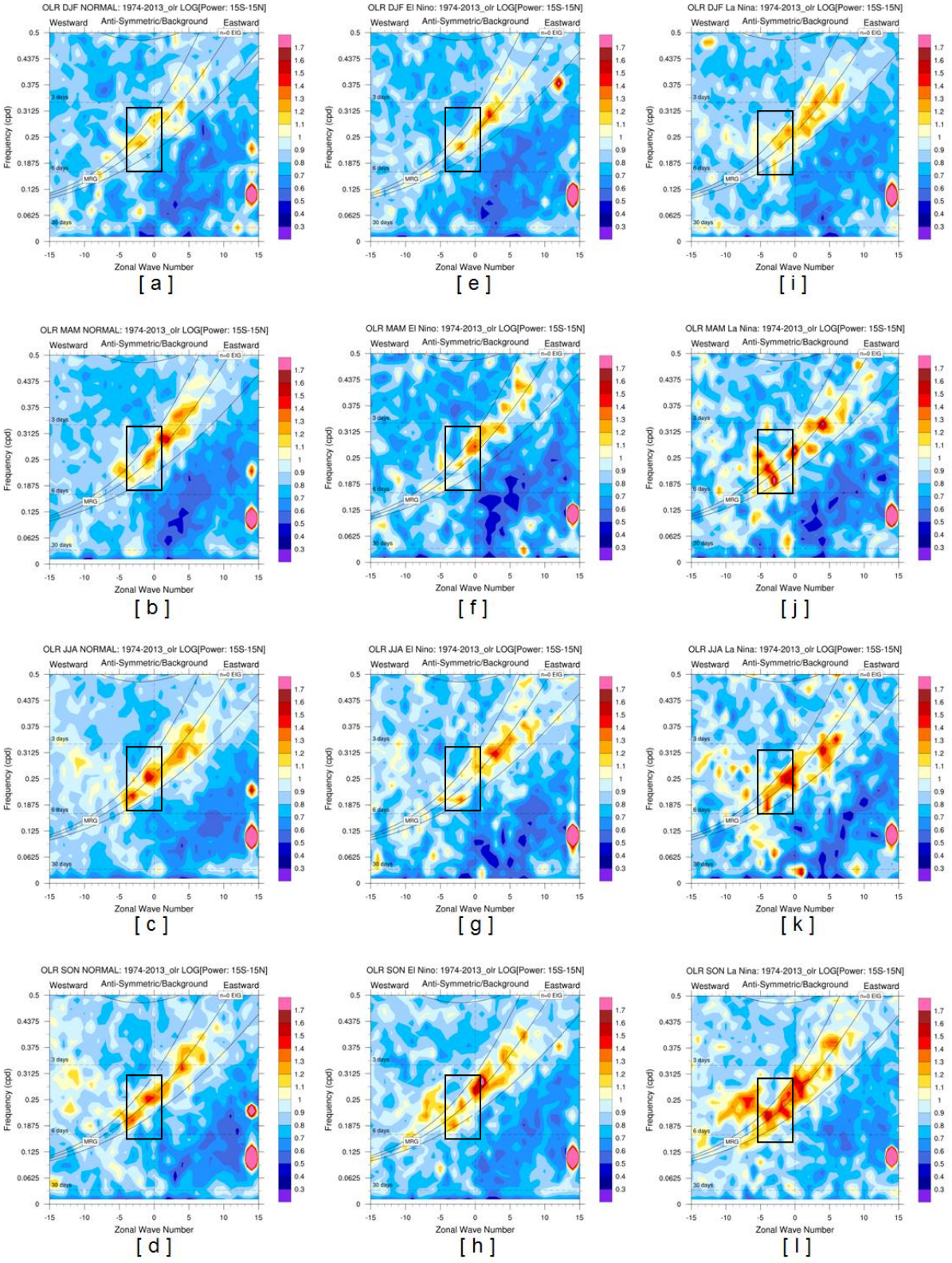

Figure 3. Anti-Symmetric STSA of outgoing longwave radiation in the normal phase (DJF (a), MAM (b), JJA (c), SON (d)), El Nino phase (DJF (e), MAM (f), JJA (g), SON (h)), La Nina phase (DJF (i), MAM (j), JJA (k), SON (l)).

Based on figure 2 and figure 3, shows that there are many waves associated with ENSO phenomenon. This wave is the result of the classification of basic types of interference waves around the equator by n integer associated with the number called nodal meridional wave mode [13]. For n = -1, commonly known as the Kelvin wave, only affects the zonal oscillations [14][4]. For n = 0, there are two groups of waves have propagation to the east and the west. The wave that moves to the east known as Inertio-waves or Gravity-wave. While the wave that spreading to the west is called Mixed Rossby-Gravity waves. This wave modes associated with antisimetry perturbation of meridional wind and equatorial relatively perturbation of meridional wind [13]. In general, for $n \geq 1$ there are three groups, namely the Rossby for the wave that move to the west and Gravity waves for the wave that move to the east and to the west [13].

Overall for each phase of ENSO, at a equivalent depth of 12-50 m to a Kelvin wave signal (n = -1) was detected in symmetrical components. Results STSA OLR at latitude 15°N-15°S shows that the Kelvin wave is detected at a frequency of approximately 0.3125 to 0.0625 cycles per day or a period of about 3.2 to 16 days by the zonal wave number 1-10 and speed phase from 10.8 to 22.1 m s^{-1}. These results are consistent with research conducted by [12][10][15]. In figure 2 symmetrical components, looks a Kelvin wave rose during ENSO phenomenon. With Kelvin wave activity in El Nino conditions are stronger than La Nina.

Kelvin waves are detected in symmetrical components for each season and for all conditions (shown in figure 2). Strong signal the presence of Kelvin wave activity occurred during DJF to MAM, were MAM as the peak. It describes the results of research conducted by [12] using the same data (OLR, years 1979-1996). Wheeler and Kiladis (1999) [12] identify EPW wave of cases in the southern hemisphere summer (November-April) and the Northern Hemisphere summer (May to October). The results showed that the Kelvin wave activity more powerful in the summer in the southern hemisphere. In that case, the results of the study of the influence of ENSO phenomenon is often stronger in the summer in the southern hemisphere (SON, DJF), at specific intervals followed by the increasing of Kelvin wave activity in the DJF to MAM period were MAM is the the strongest period of wave activity to every condition. The results according to research conducted by Huang and Huang (2011), Lubis and Jacobi (2015) 15][3], which states that the strongest Kelvin wave activity occurs during MAM period. The results further showed that compared with normal conditions, the strongest Kelvin wave activity occurs in El Nino conditions.

On the other hand, Mixed Rossby-Gravity wave (MRG, n = 0) was detected in antisymmetric components for each phase of ENSO on the selected depth equivalent 12-50 m (figure 3). Results of STSA OLR at latitude 15°N-15°S shows that the MRG wave detected at a frequency of approximately from 0.3125 to 0.1875 cycles per day, or about 3.2 to 5.3 daily periods by zonal wave numbers is 1-5 and phase speed of 10.8 to 22.1 m s^{-1}. These results are consistent with research conducted [16][12][3]. In figure 3 antisymmetric component, MRG visible wavelength obtained during La Nina.

Overall, MRG waves detected at antisymmetric component for each season and for all conditions. Indicates the presence of a strong MRG wave activity in the MAM and SON period with SON period as the peak. It describes the results of research conducted by the MRG. WK99 show that wave activity more powerful in the summer in the northern hemisphere. The results according to research conducted by [15][3] which states that the strongest activity of MRG waves occur during the SON. The results further showed that compared with normal conditions, the strongest MRG wave activity occurred in La Nina conditions.

3.3. Difference of STSA (outgoing longwave radiation field)

Differences in the power spectrum of Kelvin waves and MRG wave on El Nino and La Nina conditions for the each season is shown in figure 4. Dominance of wave spectrum on the symmetric component represented by the red color were MAM period is the strongest event. That means the power of Kelvin wave in the MAM period in El Nino conditions is stronger than other periods. While the antisymmetric component of the wave spectrum dominance shown by the blue color and the

strongest in the period MAM which means that MRG wave at MAM period of La Nina conditions are stronger than other periods.

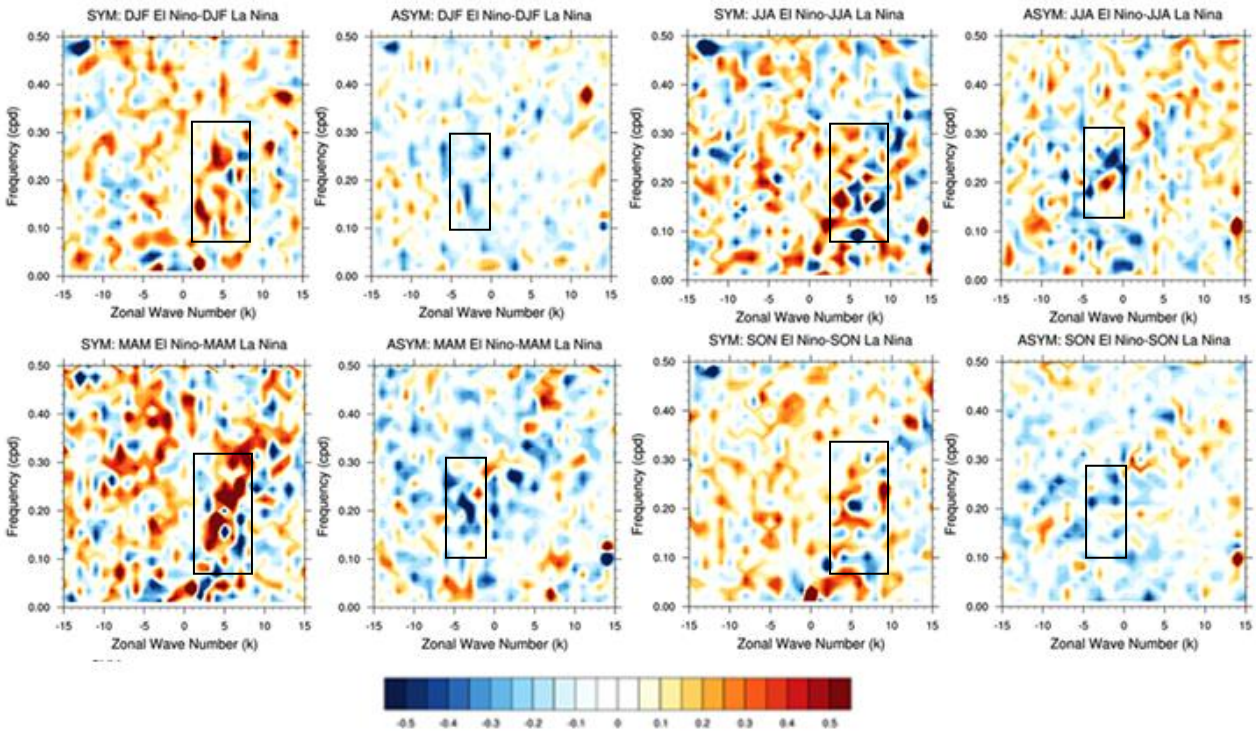

Figure 4. Difference of power spectrum in outgoing longwave radiation between El Nino and La Nina phases.

3.4. Spatial Distribution of Kelvin Wave and Mixed Rossby-Gravity (MRG) at each phase of ENSO

Spatial distribution profile of EPW, in this case the wave Kelvin and MRG not afford shown by STSA OLR. The profile is obtained by calculating the value of the variance results of each wave filter according to the method performed by [3]. Large variance stating how large wave activity in a region. Spatial distribution of Kelvin and MRG wave at each phase of ENSO is shown in figure 5. Kelvin wave activity more powerful than MRG wave. This is indicated by the value of the variant Kelvin wave is larger than the MRG wave (Varian Kelvin wave reached 20.5 (Watt m^{-2})^2, while MRG wave only 10 (Watt m^{-2})^2).

Kelvin wave spatial distribution is shown in figure 5a. These results have compatibility with research conducted by [12][15][3]. Kelvin wave spatial distribution of the strongest normal conditions occur in three regions covering the Indian Ocean (90°E), the Pacific ITCZ (5-12°N), and the Atlantic Ocean to Africa, South America (0-5°N). In the period from DJF to MAM. In El Nino conditions, the activity is centered in the middle of the Pacific Ocean to the east (90-150°W). At the La Nina conditions the strongest wave activity in the Atlantic Ocean south America to Africa (0-5°N) occurred in the MAM period.

MRG wave spatial distribution is shown in figure 5b. In this figure shows that the spatial distribution of MRG wave is divided into north and south equatorial Pacific around latitude 8°, with activity in the northern hemisphere is stronger than in southern [12][3]. In normal conditions, these waves are very weak activity with the distribution pattern in the north and south equatorial Pacific (120°E-90°W). In El Nino conditions, the activity is slightly increased compared to normal conditions and centered in the northern equatorial Pacific Ocean (120°E-90°E) in the JJA up to SON period. At

the La Nina conditions are very strong wave activity in the north and south of the equator of the Pacific in the period MAM and SON.

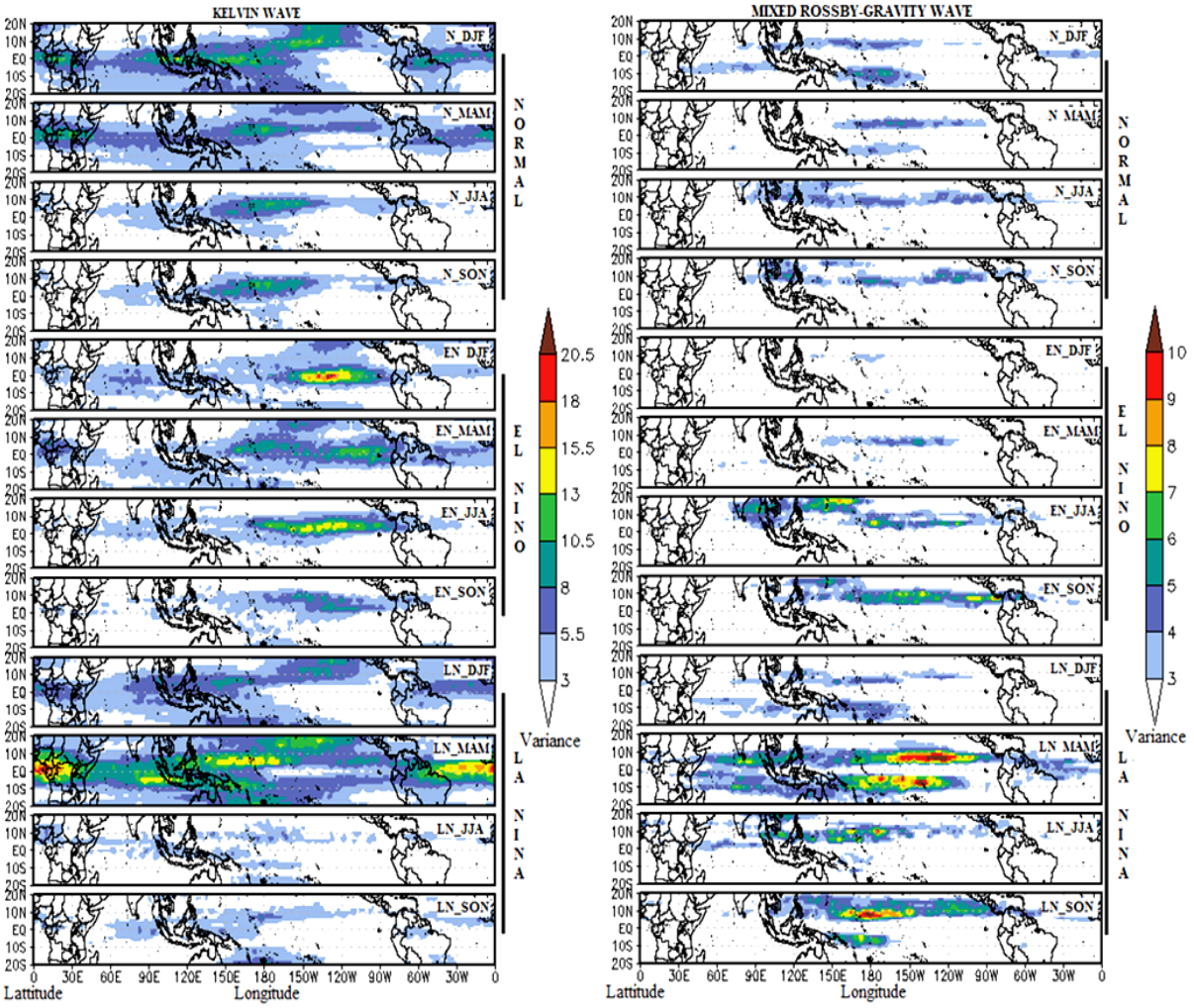

(a) (b)

Figure 5. Spatial distribution of Kelvin wave (a) and Mixed Rossby-Gravity (b) wave on Normal, El Nino and La Nina condition.

According to Holton (2004)[4], is one of convective heating plant wave activity. In connection with this, the ENSO phenomenon is a phenomenon that is closely associated with changes in regional centers convection due to warming sea surface temperatures will be analyzed for compliance with regional centers of activity EPW wave height. The suitability of the spatial distribution patterns Kelvin and MRG waves with convection activity described in the following sections.

3.5. Factors affecting Seasonal Variations Kelvin wave and Mixed Rossby-Gravity (MRG) wave at each phase of ENSO

ENSO phenomenon is closely related to a shift in the central area of convection activity and subsidence as a result of the warming and cooling of the Pacific sea surface temperature [17]. The event signal profile illustrated with OLR anomalies [2][3]. The focus of study in this research is convection. This relates to the statement [4], the formation of the cloud will generate waves.

Seasonal variations Kelvin waves and Mixed Rossby-Gravity (MRG) waves at every phase of ENSO suspected to be affected by seasonal variations in convection activity shown in the Walker circulation (figure 6a) and the profile of OLR anomalies (figure 6b) due to seasonal variations in

heating and cooling of the sea surface temperature (figure 6c) in each ENSO phase. Convection activity is indicated by negative anomalies of vertical velocity (blue in figure 6a), as proof of the existence of convection signal (negative anomalies of OLR blue in figure 6b), due to the warming of the sea surface temperature (red in figure 6c).

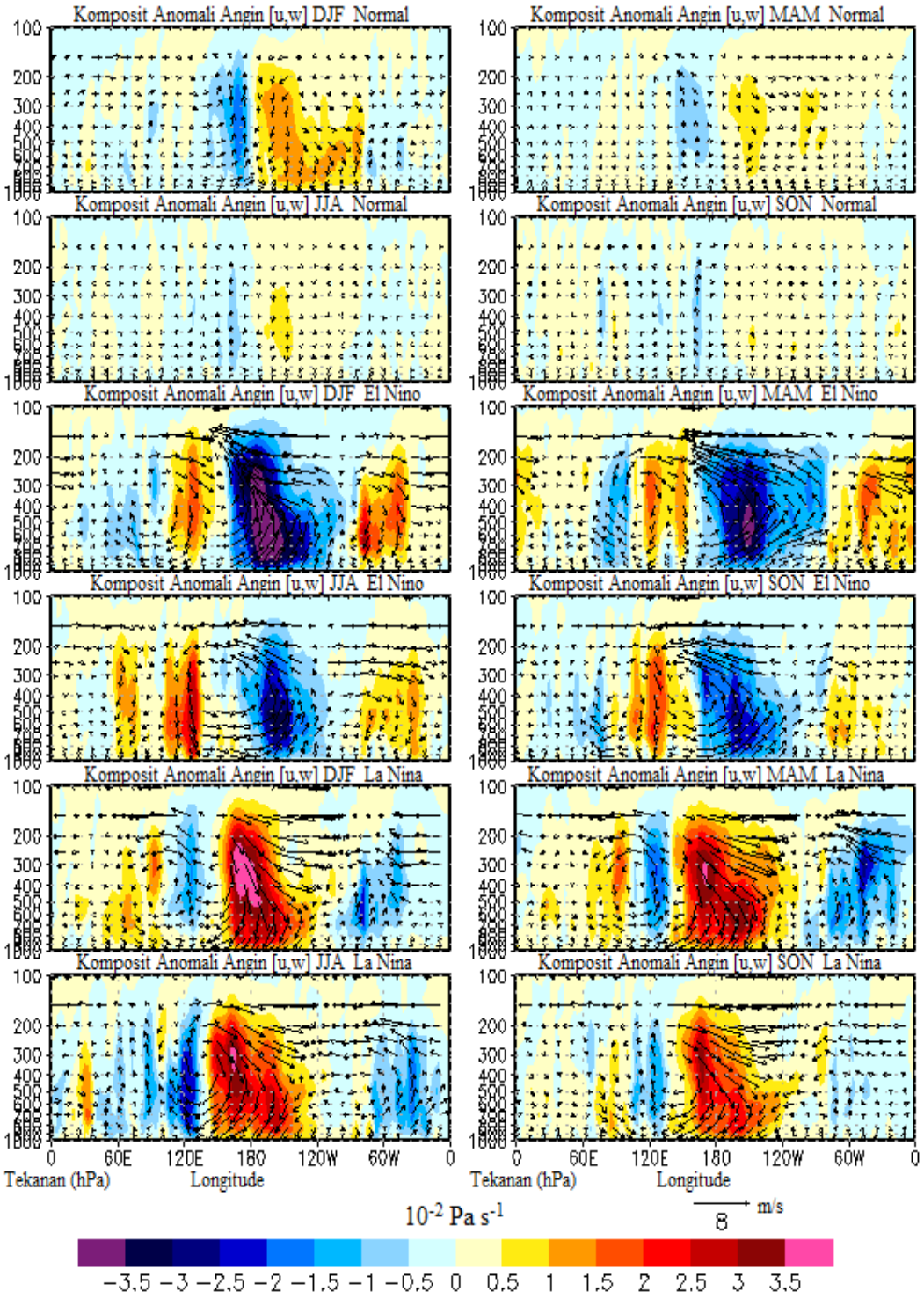

(a)

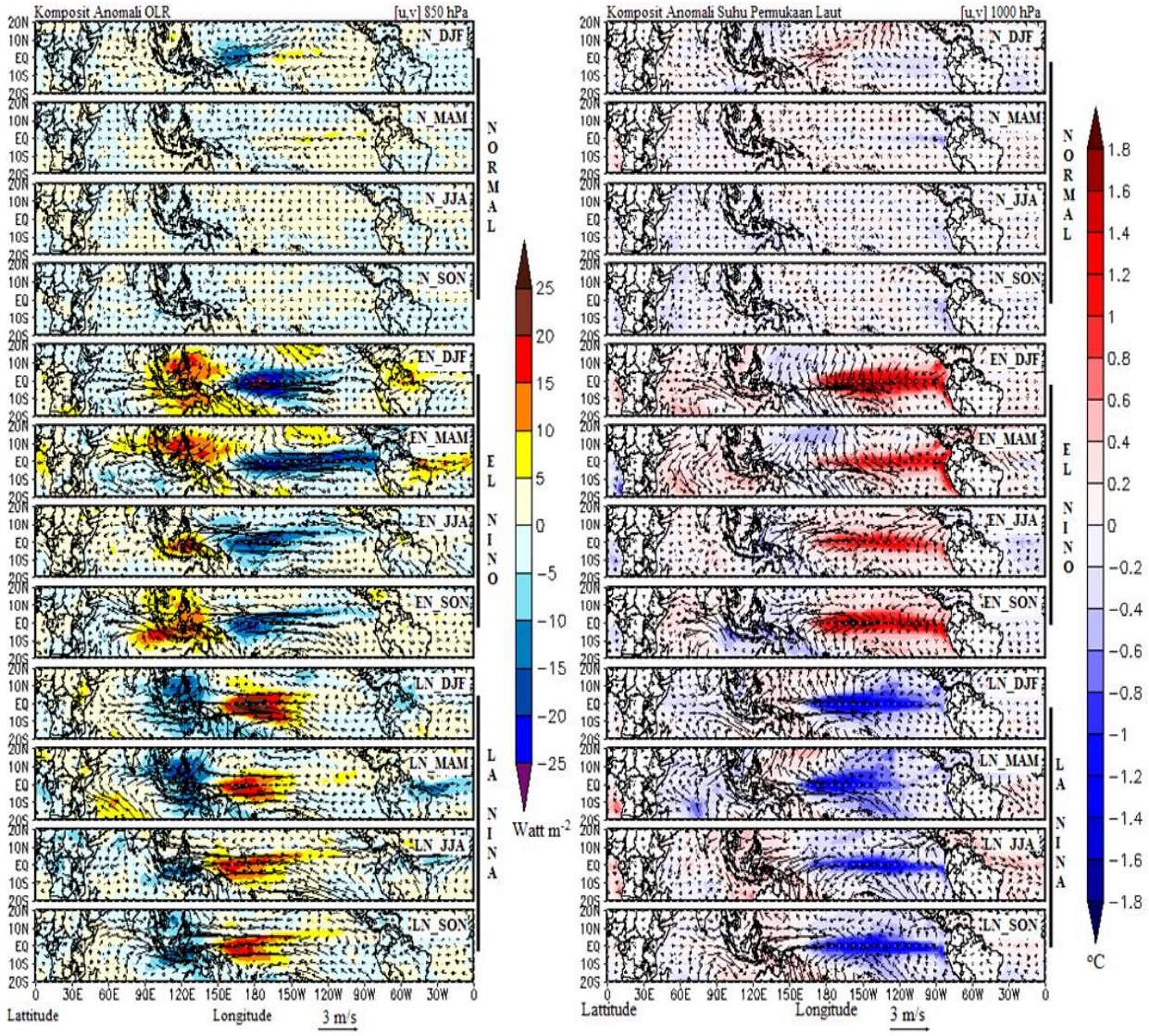

Figure 6. Seasonal Composite of vertical velocity (Pa s^{-1}), OLR (Watt m^{-2}), and SST (^{o}C) Normal condition, El Nino and La Nina. Anomalies calculated from the monthly average of the year 1982 to 2013.

Overall, convection activity for each season in each phase of ENSO indicated by Walker circulation anomaly profile (Figure 6a) have compatibility with convection signal shown by OLR profile (figure 6b). Likewise with patterns of warming and cooling of the sea surface temperature (figure 6c) behind the convection activity. There is a lag between SST anomalies seen with OLR anomalies and Walker circulation. It is seen from the incident phase of the strongest El Nino conditions and the La Nina that occurs in the SON and DJF period followed by convective signal and Walker circulation strong at DJF and MAM period. Similarly, the pattern of warming and cooling of sea surface temperatures MAM and JJA period will be followed by convection and circulation signal corresponding Walker circulation. As for normal conditions, do not see the lag time between the heating and cooling of the sea surface temperature OLR anomaly and the Walker circulation.

Based on the above, the mechanism of wave generation Kelvin and MRG can simply be explained as follows. The existence of the warming and cooling of the sea surface temperature (phases of ENSO, figure 6c) at specified intervals will increase the convection activity indicated by the presence of

convective signal amplification. Convective signal profile shown by OLR anomalies (figure 6b) and is evidenced by convection shown into the Walker circulation anomaly profile (figure 6a). Activities convection underlying wave generation Kelvin and MRG indicated by symmetric and antisymmetric components shown by STSA OLR (figure 2 and 3) and their spatial distribution is obtained by displaying the results of calculation of variance. The higher the value of the variant in a region showing increasingly strong wave activity in the region (figure 5a and 5b).

4. Conclusion

We have examined the impact of ENSO on seasonal variation of Kelvin waves and MRG waves by using NOAA outgoing longwave radiation (OLR) dataset and SST. The Kelvin waves ad MRG waves have been isolated by using space-time spectral analysis (STSA) and composite analysis. The key results are summarized as follow:

(1) ENSO phenomenon significantly influences seasonal variation of Kelvin and MRG wave activity.
(2) Kelvin waves are stronger during El Nino years with frequency of about 0.3125-0.0625 cpd (T: 3.2-16 day), zonal wave number k=1-10, and phase speed of about 10.8-22.1 m/s.
(3) MRG waves are stronger during La Nina years with frequency of about 0.3125-0.1875 cpd (T: 3.2-6 day), zonal wave number k=(-1)-(-5), and phase speed of about 10.8-22.1 m/s.
(4) The strongest Kelvin wave activity during El Nino years occurs in MAM periods, while MRG wave during La Nina years occurrs in MAM and SON periods.
(5) Maximum activity of Kelvin wave activity is observed over the central to the east Pacific in the El Nino years, while MRG wave activity are observed over the northern and southern Pacific during La Nina years.

The local variation in Kelvin waves and MRG waves is to be likely controlled by the variation in the lower level convection due to warming in sea surface temperatures over these regions. It is indicated by a shift in the center of convection activity towards the central Pacific to the east following the shift in Kelvin wave acitivity. While increase in wave activity MRG are more related to the convection over the the northern and southern equatorial Pacific ocean. The results of this study is expected to improve the prediction skill of the intra-seasonal climate in the tropicas based on the knowledge of atmosphere-ocean coupled mechanism. Further studies are required to investigate in more detail how tropical ocean influence the generation of Kelvin waves and MRG waves in opposite ENSO phase and their associated implication on surface climate.

Acknowledgment

We thank NOAA for providing the OLR, OISST, zonal and meridional wind (u,v) and vertical velocity (ω) dataset that used in this study.

References

[1] Holton JR. and RS Lindzen 1968 *Monthly Weather Review* **96** 385
[2] Kiladis G, Wheeler M, Haertel P, Straub K, Roundy P 2009 Convectively coupled equatorial waves. *Review Geophys* **47**
[3] Lubis SW and Jacobi C 2015 The modulating influence of convectively coupled equatorial waves (CCEWs) on the variability of tropical precipitation *Int. J. Climatol.* **35** 1465–1483
[4] Holton JR 2004 *An Introduction to Dynamics Meteorology* Ed ke-4. Burlington: Elsevier
[5] Dima IM and Wallace JM 2006 Structure of annual mean equatorial planetary waves in the ERA-40 Reanalyses *J.Atmos.Sci*. **64** 2862-2880
[6] Gill A E 1980 Some simple solutions for heat-induced tropical circulations *Quart. J. Roy. Meteor.Soc*. **106** 447-462
[7] Lau KM and L Peng 1987 Origin of low-frequency (intra-seasonal) oscillation in the tropical atmosphere. Part I: Basic theory *J. Atmos. Sci*. **44** 950-972

[8] Bjerknes J 1969 Atmospheric Teleconnections from the Equatorial Pacific *Mon. Weather Rev.* **97** 163 172
[9] Mc Bride J. Haylock M.R and Nicholls N 2003 Relationships between the Maritime Continent Heat Source and the El Nino-Southern Oscillation Phenomenon *J. Climate*. **16** 2905-2914
[10] Yang Gui-Ying and Hoskin B 2013 Enso Impact on Kelvin Waves and Assosiated Tropical Convection *J. Atmos Sci*. **70** 3513-3532
[11] Liebmann B. and C.A. Smith 1996 Description of a Complete (Interpolated) Outgoing Longwave Radiation Dataset *Bulletin of the American Meteorological Society* **77** 1275-1277
[12] Wheeler M and Kiladis GN 1999 Convectively coupled equatorial waves; analysis of clouds and temperature in the wave-number-frequency domain *J Atmos Sci* **56** 374-399
[13] Yanai M and Marukami M 1970 Spectrum analysis of symmetric and antisymmetric equatorial waves *J. Atmos. Sci*. **48** 331-347
[14] Matsuno T. 1966 Quasi-geostrophic motions in equatorial area *J Meteor Soc Japan.* **44** 25-43
[15] Huang P and Huang R 2011 Climatology and interannual variability of convectively coupled equatorial waves activity *J. Climate*. **24** 4451-4465
[16] Yanai M and T Maruyama 1966 Stratospheric wave disturbances propagating over the equatorial Pacific J. Meteor.Soc.Japan **44** 291-294
[17] Chiodi A M and Harrison D E 2015 Global Seasonal Precipitation Anomalies Robustly Associated with El Nino and La Nina Events-An OLR Perspective *J. Climate*. **28** 6133-6159